ACS Infectious Diseases

Article

pubs.acs.org/journal/aidcbc

Central Role of the Copper-Binding Motif in the Complex Mechanism of Action of Ixosin: Enhancing Oxidative Damage and Promoting Synergy with Ixosin B

M. Daben J. Libardo,[†] Vitaliy Y. Gorbatyuk,[†,‡] and Alfredo M. Angeles-Boza*[,†]

[†]Department of Chemistry, University of Connecticut, Unit 3060, 55 North Eagleville Road, Storrs, Connecticut 06269, United States

[‡]Biotechnology and Bioservices Center, University of Connecticut, Unit 3149, 91 North Eagleville Road, Storrs, Connecticut 06269, United States

Supporting Information

ABSTRACT: Ticks transmit multiple pathogens to different hosts without compromising their health. Their ability to evade microbial infections is largely a result of their effective innate immune response including various antimicrobial peptides. Therefore, a deep understanding of how ticks (and other arthropod vectors) control microbial loads could lead to the design of broad-spectrum antimicrobial agents. In this paper we study the role of the amino-terminal copper and nickel (ATCUN)-binding sequence in the peptide ixosin, isolated from the salivary glands of the hard tick *Ixodes sinensis*. Our results indicate that the ATCUN motif is not essential to the potency of ixosin, but is indispensable to its oxidative mechanism of action. Specifically, the ATCUN motif promotes dioxygen- and copper-dependent lipid (per)oxidation of bacterial membranes in a temporal fashion coinciding with the onset of bacterial death. Microscopy and studies on model membranes indicate that the oxidized phospholipids are utilized as potential targets of ixosin B (another tick salivary gland peptide) involving its delocalization to the bacterial membrane, thus resulting in a synergistic effect. Our proposed mechanism of action highlights the centrality of the ATCUN motif to ixosin's mechanism of action and demonstrates a novel way in which (tick) antimicrobial peptides (AMPs) utilize metal ions in its activity. This study suggests that ticks employ a variety of effectors to generate an amplified immune response, possibly justifying its vector competence.

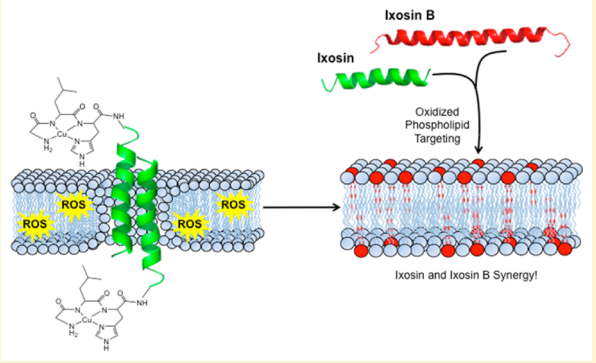

KEYWORDS: *antimicrobial peptide, tick, synergy, confocal microscopy, copper*

The rise of antibiotic resistance is a major problem in healthcare that threatens the effective prevention and treatment of an increasing number of infections caused by bacteria, viruses, and fungi. Due to their broad-spectrum antimicrobial and antifungal potency, antimicrobial peptides (AMPs) constitute an important model for the design of novel antibiotics.[1] AMPs are an essential component of the innate immune response and serve as natural antibiotics to multicellular organisms. These peptides exert their action by direct interaction with pathogens and through pleiotropic immune functions.[2]

Ticks are one of the most important arthropod vectors of human diseases; however, they have the ability to control infections when challenged with various pathogens.[3] Unlike vertebrates, ticks lack an adaptive immune system, which indicates that the mechanisms by which microbial loads are maintained at a tolerable level solely depend on phagocytic cells and their humoral response including AMPs.[3−5] Most of what is known about tick immune response comes from experiments on phagocytes found in their hemocoel, including granulocytes and plasmatocytes. More recently, many AMPs with novel functions have been isolated from various tick species, most notable of which is microplusin.[6] This 10 kDa peptide expressed in hemocytes of the cattle tick *Rhipicephalus (Boophilus) microplus* was found to starve bacteria of copper(II) ions, an essential micronutrient, most likely by sequestering copper from oxidases.[6] Furthermore, hemoglobin fragments produced by various proteases in the tick midgut have been implicated to produce reactive oxygen species (ROS), which may help control bacterial levels.[3,7,8] Although its importance is mostly overlooked, tick saliva contains multiple bioactive molecules that participate in immune modulation and inflammatory responses in the host−vector interface.[9] A survey of genetic data revealed that of the 14 AMPs expressed by various species of ticks belonging to the genus *Ixodes*, 7 are secreted in the salivary glands.[5] This information, coupled with the fact that AMPs have a large diversity of mechanisms,

Received: September 15, 2015
Published: December 5, 2015

DOI: 10.1021/acsinfecdis.5b00140
ACS Infect. Dis. 2016, 2, 71−81

Table 1. Sequence and Calculated Helicity of the Designed Peptides

peptide name	sequence	% conformations[a] in 3:1 POPE:DOPG LUVs[b] (in TFE[c]) % α-helix	% β-sheet
ixosin [Cu-ixosin]	GLHKVMREVLGYERNSYKKFFLR	14 (50) [13 (50)]	34 (11) [33 (10)]
ixosin H3A	GLAKVMREVLGYERNSYKKFFLR	16 (50)	31 (10)
ixosin$_{4-23}$	KVMREVLGYERNSYKKFFLR	11 (32)	40 (18)
ixosin$_{1-18}$ E8K, E13L, S16V/ixosin-*pch*	GLHKVMRKVLGYLRNVYK	9 (62)	44 (8)
ixosin$_{1-18}$ H3A, E8K, E13L, S16V/ixosin-*pch*-H3A	GLAKVMRKVLGYLRNVYK	14 (63)	45 (7)
ixosin$_{4-18}$ E8K, E13L, S16V/ixosin-*pch*$_{4-18}$	KVMRKVLGYLRNVYK	10 (50)	42 (11)

[a]CD spectra were deconvoluted and percent helix was calculated using the software CDNN. [b]Large unilamellar vesicles were composed of 3:1 mol ratio of POPE:DOPG suspended in 20 mM MOPS buffer, pH 7.4. [c]Percent helix in TFE was obtained at 50% (v/v) 50 mM sodium phosphate buffer, pH 7.4, and 50% trifluoroethanol.

Table 2. Antimicrobial and Cytotoxic Activity of the Peptides under Study

peptide	minimum inhibitory concentration,[a] μM: bacterium *S. aureus*	*E. coli* (MG1655)	*P. aeruginosa*	fungus *C. albicans*	geometric mean[b]	% cell viability (@ MIC vs *E. coli*) HeLa	HEK293
ixosin	64	16−32	128	16−32	53.8	91 ± 14	107 ± 6
ixosin H3A	64	16	128	64*[a]	53.8	92 ± 13	101 ± 8
ixosin$_{4-23}$	>128*	128*	>128	128*	128	81 ± 2	100 ± 14
ixosin-*pch*	8*	1*	8*	8*	4.7	76 ± 8	86 ± 17
ixosin-*pch*-H3A	4−8	2−4#	8	16−32#	9.5	72 ± 27	77 ± 15
ixosin-*pch*$_{4-18}$	128#	2	32	32	22.6	81 ± 8	85 ± 3

[a]*, $P < 0.05$ when compared to ixosin; #, $P < 0.05$ when compared to Ixosin-*pch*. MICs presented are the range of MICs obtained from three independent trials. [b]When MIC > 128 μM, the value 128 was used to calculate the geometric mean.

suggests that ticks may employ a variety of AMPs that act synergistically to amplify their immune response.

Ixosin is a 23 amino acid AMP isolated from the salivary glands of the hard tick *Ixodes sinensis* with the following amino acid sequence: GLHKVMREVLGYERNSYKKFFLR.[10] Interestingly, unlike other AMPs isolated from ticks, ixosin does not have a cysteine residue in its primary structure. Moreover, ixosin contains basic and acidic residues in the *i*- and *i*+1 positions analogous to α-defensins expressed by higher vertebrates.[11] Ixosin has shown activity against *Escherichia coli*, *Staphylococcus aureus*, and *Candida albicans* with minimum inhibitory concentrations (MICs) in the micromolar range.[10] Our group is particularly interested in the bioactivity of ixosin due to the presence of the amino-terminal copper and nickel (ATCUN) binding motif Gly-Leu-His in its sequence.

The ATCUN motif, H_2N-AA_1-AA_2-His, is a structural feature present in proteins that bind copper and nickel ions through a free NH_2-terminus, a histidine residue in the third position, and two backbone amide groups from residue AA_2 and histidine.[12] It is commonly found in proteins that interact with metal ions such as albumins and protamins. Of direct relevance to this study is that several naturally occurring AMPs contain an ATCUN motif (ATCUN-AMP). These ATCUN-containing AMPs have been purified from plants,[13] invertebrates,[14,15] and vertebrates.[16−20] We and others have attached ATCUN motifs to AMPs and showed that the resulting conjugates have higher antimicrobial activity as compared to the original AMPs.[21−24] The increase in antimicrobial activities upon the addition of the ATCUN motif is due to the ability of the AMPs to produce ROS after forming a complex with copper ions.[22,24] Whereas this increase in activity can be attributed to the addition of an exogenous peptide domain imparting a new function to the peptide, the same cannot be said directly of naturally occurring AMPs already containing this motif. The fact that ATCUN-AMPs are ubiquitous in nature (vide supra) may represent a generalized form of defense by multicellular organisms. Herein we study the function of the ATCUN motif in ixosin and how it contributes to its overall activity.

In this work, we probe several molecular determinants of ixosin bioactivity (including hydrophobicity and cationic character) with a strong emphasis on the role of the ATCUN motif. Systematic residue substitutions and deletions at the copper binding site and key positions throughout the peptide were done to piece out the individual contributions of the aforementioned structural properties. Our results reveal that whereas the ATCUN motif is not essential in the potency of ixosin, it is found to be necessary for its mechanism of action. A dramatic difference was seen in the oxygen- and copper-dependent activity of the ATCUN-containing and ATCUN-free derivatives, suggesting that wild-type (WT) ixosin kills bacteria via direct oxidative pathways. This oxidative damage was found to be exploited by another tick salivary gland AMP, ixosin B, resulting in a synergistic action between the two peptides involving the localization of ixosin B to the membrane. Notably, the cooperative interaction between ixosin and ixosin B is the first example of synergy observed among natural antimicrobial peptides.

RESULTS AND DISCUSSION

Sequence, Antimicrobial Activity, and Cytotoxicity of the Designed Peptides. We sought to determine the contribution of the copper-binding sequence in ixosin to the peptide's bioactivity. We systematically varied the sequence by substitutions and deletions of residues at and around the ATCUN motif and then measured their respective MICs against a panel of microbes. First, we synthesized the WT ixosin

DOI: 10.1021/acsinfecdis.5b00140
ACS Infect. Dis. 2016, 2, 71−81

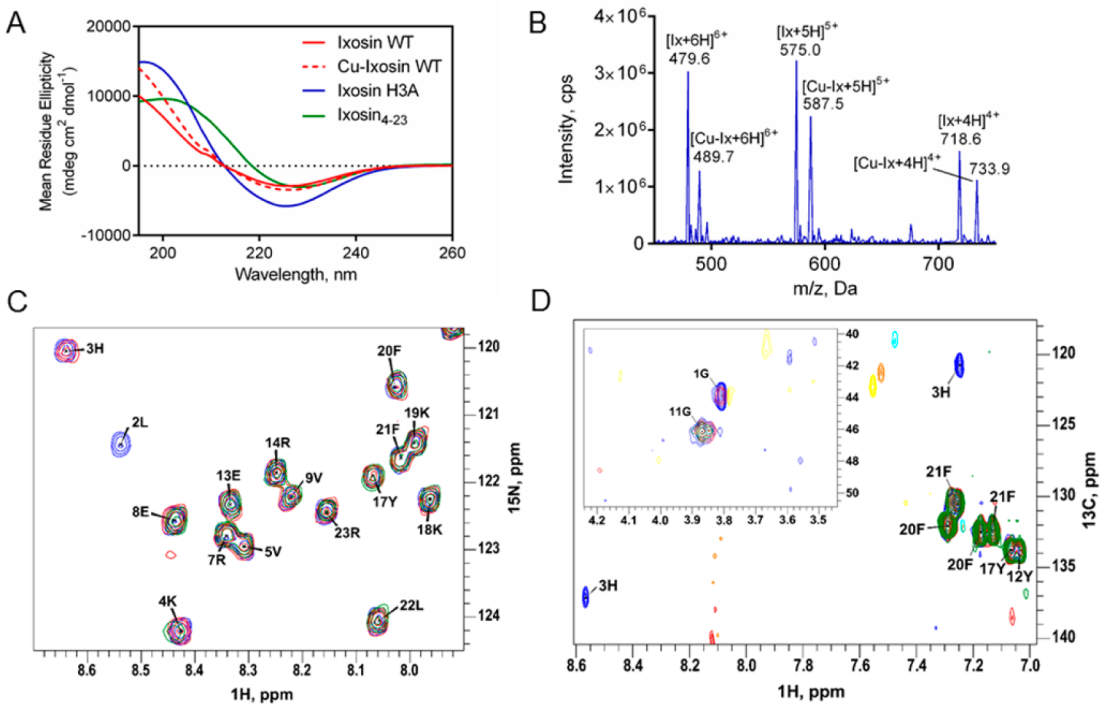

Figure 1. Ixosin conformation and Cu^{2+}-binding site studied spectroscopically. (A) CD spectra obtained in the presence of 3:1 POPE:DOPG LUVs at a peptide:lipid ratio of 1:30. The curves resemble a hybrid spectra with contributions from α-helix and β-sheet. (B) ESI-MS spectra of Cu-ixosin WT complex showing 1:1 binding stoichiometry. (C) $^{1}H-^{15}N$ HSQC and (D) $^{1}H-^{13}C$ HSQC spectra of free ixosin (blue), 1:5 ratio of Cu^{2+}:ixosin WT (red), and 1:2 Cu^{2+}:ixosin WT ratio (green) recorded in 93% 20 mM acetate buffer, pH 4.4, and 7% D_2O. NMR spectra indicate that ixosin WT binds to Cu^{2+} via its ATCUN sequence.

and its H3A mutant (to abolish copper binding, Table 1) and found that they had equal potencies (from the geometric mean of MICs, Table 2). When the ATCUN motif was completely deleted ($ixosin_{4-23}$), the potency decreased 2-fold. The minimum (H3A substitution) versus maximum (ATCUN deletion leading to loss of both a positively charged and hydrophobic residue) perturbations in ixosin's primary sequence indicate that the ATCUN motif is not essential to the peptide's potency. Our studies on truncated ixosin derivatives showed that the C-terminal region (KFFLR) is necessary for its activity (Supporting Information, Table S2) as its deletion ($ixosin_{1-18}$) completely abrogated activity. We then asked whether increasing the hydrophobicity and cationic character of $ixosin_{1-18}$ would restore its activity; therefore, we introduced three point mutations (E8K, E13L, and S16 V) to generate ixosin-*pch* (pch for plus cationic and hydrophobic, Table 1), a derivative that is an order of magnitude more potent than the WT. This result is consistent with known facts that positive charge and hydrophobicity are important factors in antimicrobial activity.[25,26] To study the contribution of the ATCUN motif to this highly hydrophobic derivative, we synthesized ixosin-*pch* derivatives harboring ATCUN mutations. We found that ixosin-*pch*-H3A was 2-fold less potent, whereas deletion of the ATCUN motif (ixosin-pch_{4-18}) decreased the potency 5-fold. This suggests that the ATCUN motif is essential for the activity of a highly positively charged and hydrophobic ixosin derivative, ixosin-*pch*.

To investigate the potential toxicity of our peptides toward mammalian cells, we employed the MTT assay. Using the cervical carcinoma cell line, HeLa and human embryonic kidney (HEK293) cells, we find that ixosin and its ATCUN-less derivatives are minimally toxic, causing only about 6−9% cell death at their tested MIC (vs *E. coli*). Ixosin-*pch* and its derivatives were found to kill up to 28% of the cellular population (Table 2 and Supporting Information, Figure S1). This result suggests a certain degree of selectivity of ixosin to target microbes.

Spectroscopic Characterization of Conformation and Cu^{2+}-Binding Site in Ixosin. The activity of AMPs is not only dependent on its primary structure but is also tightly linked to its three-dimensional shape.[26] To eliminate the possible conformational effects in the activity of ixosin and its derivatives, we determined their respective secondary structure using circular dichroism (CD) spectroscopy in two different media. First, in the presence of large unilamellar vesicles (LUVs) composed of a 3:1 mol ratio of 1-palmitoyl-2-oleoyl-phosphatidylethanolamine (POPE) to dioleoylphosphatidylglycerol (DOPG), we observed CD traces resembling a hybrid between helical and β-sheet structures (Figure 1A). We used the neural network artificial intelligence program CDNN[27] to deconvolute and calculate the contributions between different conformations and found that in the presence of a membrane environment, ixosin and its derivatives either predominantly adopt a β-sheet structure or are in an unordered state. On the other hand, in the presence of the membrane mimicking solvent, trifluoroethanol (TFE), all peptides adopt a predominant α-helical structure (Supporting Information, Figure S2). This flexibility in conformations demonstrates the ability of ixosin to respond to changes in its environment, possibly encouraging different interactions. This would be especially advantageous if ixosin is also expressed in (or circulated to) various regions of the tick body or transferred to the host during feeding (because biological composition will vary greatly), as adopting a specific secondary structure often leads

DOI: 10.1021/acsinfecdis.5b00140
ACS Infect. Dis. 2016, 2, 71−81

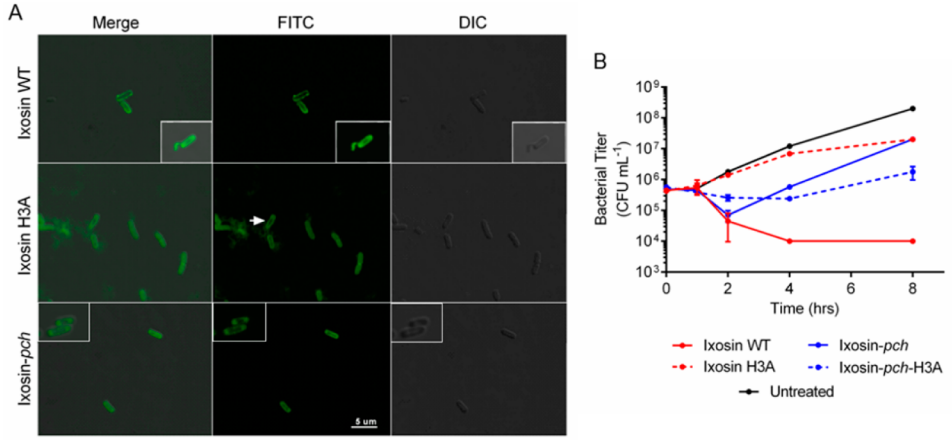

Figure 2. (A) Bacterial localization of ixosin WT (inset: ixosin WT for 1 h), ixosin H3A, and ixosin-*pch* (inset: ixosin-*pch*-H3A) revealed via laser confocal microscopy. Fluorescence micrographs show extensive membrane staining by all ixosin derivatives during a 30 min incubation period. (B) Time−kill kinetics curve of ixosin and its derivatives showing that ATCUN-containing peptides are bactericidal, whereas corresponding H3A mutants are bacteriostatic.

to a functionally active AMP. Regardless of the environment, we observed minute differences in conformations between the GLH- and GLA-containing peptides (Table 1; 1−3% for ixosin WT versus ixosin H3A and 1−5% for ixosin-*pch* versus ixosin-*pch*-H3A). This suggests that the differences in their potency are likely not a result of the extent to which they adopt their secondary structures. On the contrary, ixosin-*pch* was found to have more ordered structures compared to ixosin WT (Table 1, 5−9%), which could have contributed to their large difference in potencies. Finally, we note that metalation of ixosin WT showed a negligible change, 1%, in conformation relative to free ixosin, suggesting that copper binding neither promotes nor inhibits secondary structure formation.

When a Cu^{2+} (or Ni^{2+}) ion binds to the ixosin ATCUN motif, the backbone amide nitrogens of Leu-2 and His-3 get deprotonated to accommodate the metal in a distorted square planar geometry,[12] generating a Cu−ixosin complex having a molecular mass of 2931.96 Da. We mixed 1 equiv of ixosin WT with 0.8 equiv of Cu^{2+} and injected the mixture to an ESI-MS. We observed multiply charged species bearing m/z values consistent with a 1:1 Cu:ixosin stoichiometry (Figure 1B). The peaks attributed to $[Cu-Ix + 3H]^{3+}$ and $[Cu-Ix + 4H]^{4+}$ showed large similarities to the simulated isotopic distribution pattern (Supporting Information, Figure S3), suggesting that these peaks are not an artifact from the analysis. Furthermore, ixosin H3A did not seem to bind Cu^{2+} on the basis of our MS analysis (Supporting Information, Figure S4), indicating that His-3 is required for metal binding. We then mapped the actual copper-binding site via the heteronuclear single-quantum correlation (HSQC) approach. Upon gradual addition of Cu^{2+}, we observed signal intensity degradation for a set of protons, whereas the rest of the HSQC spectra remained unperturbed. This indicates that, except for the metal coordination site, there are no conformational changes in the peptide backbone upon Cu^{2+} complexation. We observed the loss of $^{1}H-^{15}N$ correlation starting at ratio Cu:ixosin WT of 1:5 for Leu-2 and at 1:2 for His-3 amide protons (Figure 1C). This is consistent with the deprotonation of these backbone amides upon copper binding. In addition, we monitored the $^{1}H-^{13}C$ correlations and found that at the lowest studied metal concentration (1:5 Cu:ixosin), the HSQC signals of the imidazole protons ε_1-H (~8.55 ppm) and δ_2-H (~7.25 ppm) of His-3 become undetectable, whereas signals from other aromatic residues are unchanged (Figure 1D). Furthermore, the $^{1}H-^{13}C$ correlations of the α-H of Gly-1 also disappear starting at a 1:2 ratio (inset in Figure 1D). Due to the paramagnetic nature of Cu^{2+}, any proton in its vicinity will experience a shortened transverse relaxation time leading to a significant broadening of its NMR signal.[28] Although deprotonation of the imidazole residue of His-3 and α-CH_2 of Gly-1 is not expected upon copper complexation, we believe that the bound Cu^{2+} broadened the HSQC resonances of these protons beyond recognition. At higher metal concentrations (up to 1:1 ratio), the α-H of Gly-1 and amide proton of Lys-4 broadens beyond detection as well. Taken together with our MS data, we definitively show that ixosin WT indeed binds to Cu^{2+} through its ATCUN motif and that any other potential ligands within the peptide chain do not have a high-enough affinity to compete with the N-terminal sequence. Because the motif is conserved between ixosin WT and ixosin-*pch*, we expect the two peptides to have similar Cu^{2+}-binding behaviors.

Ixosin Is a Bactericidal Peptide Localizing in the Membrane. The initial interaction between AMPs and bacteria occurs in the membrane.[29] Whereas some AMPs have been found to cross the membrane and perturb various intracellular processes,[30,31] most AMPs are membrane active.[1] To determine the bacterial localization of ixosin and its derivatives, we employed laser confocal microscopy. The 5(6)-carboxyfluorescein-labeled peptides were synthesized on resin by coupling the dye to the ε-amino group of Lys-18; this was done to preserve copper binding (whenever possible) in the N-terminal as a free $-NH_2$ group is required.[12] Thirty minutes postexposure to the peptides at their MIC, we observed fluorescent hollow ellipsoids indicative of membrane localization for ixosin WT, ixosin-*pch*, and their respective H3A derivatives (Figure 2A). Furthermore, green fluorescence was not found to colocalize with blue fluorescence from Hoescht 33342, a DNA tracer (Supporting Information, Figure S5). These results also resemble our reported observations on anoplin, a membrane-binding AMP.[22] A closer examination of the ixosin H3A panel shows some cells stained homogeneously, whereas others appear as hollow ellipsoids (indicated by the white arrow). This observation is consistent with the model of self-induced peptide uptake where AMPs (and other cell-

DOI: 10.1021/acsinfecdis.5b00140
ACS Infect. Dis. 2016, 2, 71−81

penetrating peptides) generate transient pores, which they use to cross the membrane and equilibrate its concentration.[29,32] We also observed this for ixosin WT when incubated for 1 h as more intracellular staining was observed (inset in Figure 2A). Our microscopy studies revealed that the structural changes we applied to ixosin did not significantly alter its localization during the time scale of our experiments.

Increasing evidence suggests that initial membrane binding and destabilization caused by AMPs at their MICs is not the determining factor for cell death.[33−35] To investigate this, we looked at the killing kinetics of ixosin and its derivatives (Figure 2B). We found that at the MIC, ixosin WT is bactericidal (decreasing bacterial content by 2 orders of magnitude at the first 4 h) with cell death commencing 1 h postexposure. On the other hand, ixosin H3A exhibited a weak bacteriostatic effect at its MIC. Taken together with our microscopy results, we believe that initial membrane localization (observed at 30 min) contributes negligibly to cell death as bacterial population was relatively constant for the first hour of incubation. In the case of ixosin-*pch*, we observed a decrease in viable bacteria followed by a steady growth beginning at 2 h. This trend was a lot less pronounced for ixosin-*pch*-H3A, where there was little fluctuation in viability over 8 h. Derivatives of ixosin WT and ixosin-*pch* containing D-amino acids were also found to be bactericidal (Supporting Information, Figure S6). Our time−kill kinetics results suggest that the ATCUN-containing peptides are bactericidal at their MIC, whereas their corresponding H3A mutants are bacteriostatic. This dramatic change in mechanism arising from a single amino acid substitution suggests the possibility that ATCUN-containing ixosin derivatives, apart from membrane binding and destabilization, may utilize an independent pathway that may be more destructive to the cell.

Activity of ATCUN-Containing Derivatives Are Dependent on Cu^{2+} and O_2 Levels. Our time−kill kinetics studies suggested the involvement of the ATCUN motif in the bactericidal action of ixosin. The Cu−ATCUN complex has repeatedly been shown to form ROS in combination with biologically relevant reducing agents.[36−38] Given that the ROS production by the ATCUN motif requires the presence of both Cu^{2+} and O_2 (eqs 1−3, L = ATCUN),[36] we next asked whether their concentration affects the activity of ixosin and its derivatives.

$$2L{-}Cu^{II} + O_2 + 2e^- \rightarrow L{-}Cu^{II}{-}O{-}O{-}Cu^{II}{-}L \quad (1)$$

$$L{-}Cu^{II}{-}O{-}O{-}Cu^{II}{-}L \rightarrow 2L{-}Cu^{II} + HO_2^- \quad (2)$$

$$2L{-}Cu^{II} + HO_2^- + H^+ + e^- \rightarrow 2L{-}Cu^{II}{-}OH + OH^- \quad (3)$$

We studied the activity of ixosin and its derivatives with and without copper chelators (Figure 3A) and under normal- and low-oxygen levels (Figure 3B). We resuspended *E. coli* in a medium that maintains the viability of cells while inhibiting their growth (HEPES minimal medium);[39] this allowed us to have a baseline bacterial count per trial. Then, we exposed the cells to peptides at their MIC, followed by incubation for 2 h and then plating in LB agar for colony enumeration. We reasoned that a decrease in copper or oxygen levels will lead to fewer ROS formed and hence will result in lower potency. We observed a marked increase in the number of colonies when the copper chelator triethylenetetramine (TETA) or penicillamine ($PennNH_2$) was added and when oxygen was depleted (Figure S7). This indicates that individual depletion of copper or

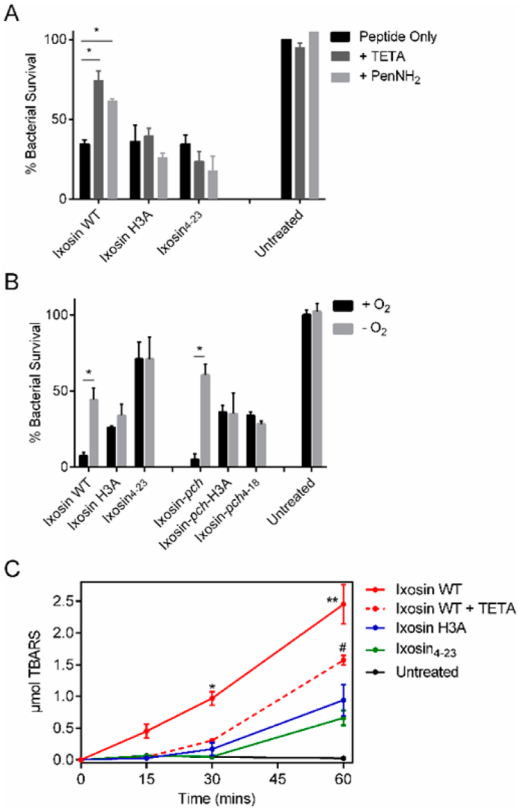

Figure 3. Oxidative activity of ixosin is due to the presence of ATCUN motif. (A) Bacterial survival was determined in the presence of copper chelators, triethylenetetramine (TETA) and penicillamine ($PenNH_2$). Data highlight importance of Cu^{2+} to activity of ixosin WT. (∗) $P < 0.05$. (B) Activity of ixosin and derivatives under normoxic (+ O_2) and hypoxic (− O_2) conditions. Data show role played by O_2 in the activity of ATCUN-containing peptides suggesting a possible involvement of ROS. (∗) $P < 0.01$. (C) Extent of lipid peroxidation promoted by ixosin measured over the first hour of incubation and calculated as micromoles of thiobarbituric acid reactive substances (TBARS). A significant increase in peroxidized lipids by ixosin WT was observed, indicating a major role in its activity. (∗ and #) $P < 0.005$; (∗∗) $P < 0.001$.

oxygen rescued the growth of bacteria when exposed to ATCUN-containing peptides; that is, the ATCUN-containing peptides were more active in the presence of copper and oxygen (Figure 3A,B). This, however, was not the case for the H3A mutants and the derivatives lacking the ATCUN motif completely. For those peptides, no statistically significant difference was observed upon Cu^{2+} or O_2 depletion. These data showed that there is indeed an involvement of ROS in the activity of the ATCUN-containing ixosin derivatives and that ROS formation may even be critical to its bactericidal property.

A closer examination of Figure 3A shows that copper chelation with 200 μM TETA did not restore ∼100% bacterial survival. Although this may be a function of competition for copper between ixosin and the copper chelator, the added TETA was in a large excess relative to the copper content of the medium (previously measured as 5 ppm, ∼78 μM)[40] and to the concentration of ixosin WT (32 μM). It can therefore be assumed that, under these conditions, most (if not all) ixosin exists in the nonmetalated form. The fact that free ixosin WT was still able to kill ∼25% of the cells (Figure 3A) suggests a pathway leading to cell death that does not involve Cu^{2+} binding. Our MIC results coupled with our mutational analysis

DOI: 10.1021/acsinfecdis.5b00140
ACS Infect. Dis. 2016, 2, 71−81

showed the relevance of hydrophobicity and cationic charge to the activity of ixosin (Table 2). Incidentally, these physicochemical properties also dictate the extent of membrane activity. Hence, as one would expect from any prototypical AMP, ixosin may also possess membrane disruption capability—a copper-independent mechanism—which leads to cell death.

ATCUN-Containing Ixosin Derivatives Peroxidize Lipids in *E. coli* Cells. Because ixosin is found to localize at the membrane and ROS is implicated in its activity, we investigated whether ixosin can oxidize the lipids in the membrane of *E. coli*. We hypothesized that the ROS formed is localized in the membrane environment and hence will target unsaturations found in the bilayer. We employed a standard assay to measure the extent of lipid peroxidation brought about by our peptides at three different time points. The peroxidation products (thiobarbituric acid reactive substances, TBARS) were then quantified using analytical HPLC (Supporting Information, Figure S8). Our data show that there is an immediate increase in peroxidized lipid following exposure to ixosin WT. This peroxidation increased sharply through the first hour of incubation. On the other hand, a lag phase was observed for ixosin H3A and ixosin$_{4-23}$, which then modestly increased after 30 min. After 60 min, lipid peroxidation by ixosin WT was 3-fold greater ($P < 0.001$) than its ATCUN-free derivatives. This coincides with the onset of bacterial killing we observed from our time−kill kinetics studies (Figure 2B). Taken together, our results suggest that oxidatively damaging the membrane may be a significant step in the bactericidal activity of ixosin. Moreover, addition of the copper chelator, TETA, led to a ∼35% reduction in lipid peroxidation (at 60 min postexposure), suggesting that peroxidation is indeed Cu^{2+}-dependent.

The MICs of the ATCUN-containing peptides were measured after pre-incubation with Cu^{2+} and found to be similar to those of the naïve peptide (data not shown). Furthermore, an attempt to boost bacterial copper content was made by growing *E. coli* in media containing 50 μM Cu^{2+} (a concentration far below its MIC, which was determined to be 1 mM). The MIC against the "copper-loaded" bacteria was also unchanged (data not shown). In contrast, the tick AMP, microplusin, was rendered inactive by exogenous Cu^{2+} in the media.[6] Silva et al. hypothesized, on the basis of their O_2 consumption experiments in the presence of cyanide and the energy uncoupler carbonyl cyanide *m*-chlorophenylhydrazone (CCCP), that microplusin might be sequestering Cu^{2+} from one or more of the heme−copper terminal oxidases[6] (members of the electron transport chain that act to reduce O_2 to H_2O). We hypothesize a distinct mechanism of action for ixosin—one that does not involve sequestration of essential copper for the following reasons: (1) There exists a pool of labile copper ions in *E. coli* (and other bacteria), most of which are found in the periplasm bound to methionine, cysteine, or glutathione.[41−43] This labile pool of copper ions is most likely in the +2 state (preferentially bound by the ATCUN motif) due to the presence of multicopper copper oxidases that act to detoxify Cu(I) by oxidizing it to Cu(II).[44] Therefore, preloading ixosin with Cu^{2+} contributes negligibly because there is plenty of labile copper that ixosin can theoretically scavenge. (2) Our normoxic and hypoxic experiment (Figure 3B) showed increased survival of ixosin-treated cells when O_2 was depleted. If ixosin bound copper belonging to a respiratory metalloprotein (or any copper-binding protein), a decrease in oxygen is expected to force the ixosin-treated cells into a metabolically impaired state (untreated cells would be in a metabolically dormant state), perhaps even pushing the cells to extreme starvation, which should lead to cell death. Hence, it is clear that even though microplusin and ixosin both seem to utilize Cu^{2+} in their activity, the manner in which they do so differs. Finally, we found that ixosin generated high levels of peroxidized lipids (Figure 3C), a phenotype expected only if the peptide is metalated. In theory, if ixosin WT did not bind copper, the amount of TBARS between ixosin WT and ixosin H3A would have been comparable. Overall, our results thus far indicate the likely possibility that ixosin is metalated in cella and that this metalation causes peroxidation of lipids in the membrane.

The ATCUN Motif in Ixosin Promotes Synergy with Ixosin B. Multiple secreted salivary gland peptide orthologs have been identified in hard ticks.[5] Because of the crucial role played by tick saliva in modulating the immune response at the host−tick interface, expression of an arsenal of salivary gland AMPs suggests possible synergistic interactions between these molecules.[45,46] Like ixosin, ixosin B (QLKVDLWGTRSGIQPEQHSSGKSDVRRWRSRY) is an AMP isolated from the salivary glands of *I. sinensis*.[47] We examined possible synergy between ixosin and ixosin B through the context of lipid oxidation. Using a 1:1 mixture of ixosin and ixosin B, we measured the fractional inhibitory concentration (FIC) index, which is assessed as FIC = [AMP1]/MIC_{AMP1} + [AMP2]/MIC_{AMP2}, where MIC_{AMP1} and MIC_{AMP2} are the MICs of AMPs 1 and 2 alone and [AMP1] and [AMP2] are the MICs of the AMPs in combination. An FIC index <0.5 indicates good synergy (representing a ≥4-fold increase in activity), whereas an FIC index of 0.5−1.0 represents additive activity. When tested against *E. coli* PDJ1, a parental strain, we found that all 1:1 peptide mixtures used exhibited additive activity (Table 3).

Table 3. Synergistic Interaction between Ixosin Derivatives and Ixosin B Expressed as the FIC[a]

	FIC index (effect[b])	
peptide	*E. coli* PDJ1	*E. coli* MWF1
ixosin WT + ixosin B	0.562 (A)	0.281 (S)
ixosin H3A + ixosin B	0.625 (A)	0.625 (A)
ixosin$_{4-18}$ + ixosin B	1.000 (A)	1.000 (A)
ixosin WT + ixosin H3A	0.750 (A)	0.375 (S)

[a]Because regulation and relative expression of ixosin and ixosin B are currently unknown, we measured FIC indices using a 1:1 mixture of both peptides. [b]Letters in parentheses indicate conclusion drawn from FIC indices: A, additive; S, synergistic.

To confirm the importance of lipid oxidation in the synergistic effect, we measured FIC indices in *E. coli* MWF1, a strain (an isogenic mutant derived from PDJ1) containing elevated levels of unsaturated fatty acids in its membrane.[48] Not surprisingly, we observed a synergistic interaction between ixosin and ixosin B, whereas the additive activity of ixosin H3A and ixosin B was preserved. Furthermore, when ixosin and ixosin H3A were mixed, a synergistic interaction was also observed, albeit to a lesser extent. These results indicate that the ATCUN motif is imperative in eliciting a synergistic interaction between ixosin and ixosin B. Moreover, the differences observed for the two *E. coli* strains indicate that membrane lipid unsaturations—a substrate for peroxidation—are a requirement for synergy.

Ixosin B Interacts Differently with Oxidized Phospholipids. It has been previously suggested that oxidized phospholipids in the lipid bilayer can be a potential target of

DOI: 10.1021/acsinfecdis.5b00140
ACS Infect. Dis. 2016, 2, 71−81

AMPs.[49,50] The amine groups from the AMP may act as nucleophiles toward the electrophilic carbonyl groups in oxidized lipids to generate Schiff bases.[51] To test whether this is a potential avenue of synergy between ixosin and ixosin B, we studied the interaction of ixosin B with model membranes by following quenching of tryptophan fluorescence as a consequence of acrylamide titration. We used 3:1 POPE:DOPG LUVs and preoxidized them using the copper complex of ixosin for 36 h. Because we were working with a purified system, we added ascorbic acid to promote ROS formation. We have previously observed that Cu−ATCUN complexes consume >90% of the ascorbic acid within the first 4 h of incubation;[21] hence, we expected no interference from exogenous ascorbic acid. Additionally, our oxidation did not alter the diameter and size distribution of the LUVs as confirmed by dynamic light scattering (Supporting Information, Figure S9). To determine the membrane interaction of ixosin B, we generated a Stern−Volmer plot from which we calculated K_{SV} (Stern−Volmer quenching constant, Figure 4), a direct measure of Trp

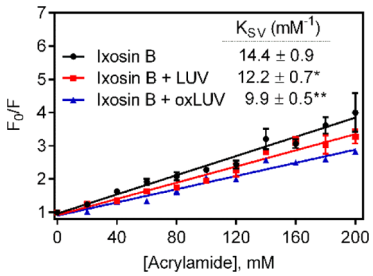

Figure 4. Decrease in tryptophan fluorescence resulting from titration with the water-soluble collisional quencher, acrylamide. F and F_0 are fluorescence intensity with and without the quencher. K_{SV} is a direct measure of solvent accessibility of Trp residues and hence a reporter of membrane interaction. The graph indicates that ixosin B has a stronger affinity toward oxidized membranes. (∗) $P < 0.01$ compared to free ixosin B; (∗∗) $P < 0.01$ compared to ixosin B + LUV.

accessibility from the aqueous environment.[49] Compared to free ixosin B, our data showed a decrease in quenching constant when native LUVs were added; furthermore, a statistically significant decrease was observed when oxidized LUVs were used. There is therefore a greater membrane interaction by ixosin B when the lipids in the membrane are oxidized. These results are consistent with the results obtained by Matilla et al. utilizing oxidized phospholipids to generate LUVs instead of oxidizing the LUVs. We note, however, that whereas Matilla et al. observed a ∼90% decrease in K_{SV}, we saw only a ∼30% difference in our experiments. This can be attributed to several factors, including LUV composition, amount of oxidized lipids in LUVs, and, more likely, the fact that ixosin B has two Trp residues close to both the N- (W7) and C-termini (W28). Whereas the relative orientation and affinity of ixosin B within the membrane is unknown, there is a slim probability that both tryptophans are projected away from the aqueous phase. This leads us to speculate on a conformation where only one is protected from acrylamide while the other is kept accessible. However, we can say with certainty that ixosin B has a stronger membrane interaction in the presence of oxidized phospholipids.

ATCUN Motif in Ixosin Causes Ixosin B To Delocalize into the Bacterial Membrane. To identify a cellular basis of the synergy between ixosin and ixosin B, we looked at their interaction in live *E. coli*. We labeled ixosin B with 5(6)-carboxytetramethylrhodamine at its N-terminal and observed its co-localization with ixosin WT and ixosin H3A. We found that ixosin B alone stains the cells homogeneously, indicative of diffusion throughout the entire cell (Figure 5). From the plot of fluorescence intensities (Figure 5B), one can see a clear co-localization of ixosin B with DNA stained by Hoechst 33342. When *E. coli* was cotreated with ixosin and ixosin B (at their FIC for 30 min), a strong co-localization between the green and red fluorescence is observed, which manifested as yellow hollow ellipsoids (Figure 5C). Furthermore, intracellular staining by ixosin B seems to have decreased, as did its co-localization with DNA (Figure 5D). This shows that in the presence of ixosin, the affinity of ixosin B to the bacterial membrane is increased. On the other hand, the intracellular localization of ixosin B was not affected by cotreatment with ixosin H3A (Figure 5C) because ixosin B again co-localized with DNA (Figure 5E). Taken together, our results demonstrate that the presence of the ATCUN motif in ixosin causes ixosin B to delocalize to the bacterial membrane, a phenomenon that (to the best of our knowledge) has not been reported to date.

Proposed Mechanism of Action of Ixosin Highlights the Central Role of ATCUN Motif. Pooling our data together, we propose a plausible mechanism of action of ixosin, the details of which are illustrated in Figure 6. Ixosin expression is induced when the tick is challenged with bacteria. Ixosin then binds copper either endogenously located in the target bacteria or from the host. Human serum albumin (also containing an ATCUN motif, Asp-Ala-His) has been proposed to function as a copper transporter with a picomolar affinity.[52] Because isolated ATCUN motifs and shorter peptides containing this sequence have been reported to bind copper with affinities in the same range (or even higher), ixosin can also compete and sequester Cu^{2+} from albumins. Once bound to copper, the complex resides in the bacterial membrane. Non-metalated ixosin residing in the membrane can sequester labile copper from the bacteria itself. Once bound to the membrane, ixosin may induce local perturbations leading to membrane disruption. With the aid of dioxygen, Cu−ixosin forms ROS, which then diffuse to and react with nearby unsaturations in the bilayer causing lipid (per)oxidation. The (per)oxidized lipids then become a target for other AMPs (including ixosin B) leading to a synergistic effect. Work is currently being done in our laboratory to elucidate the exact molecular details of the oxidized lipid targeting by ixosin B. We hypothesize, however, that if Schiff bases are indeed formed,[49] this leads to ixosin B being covalently anchored to the membrane as opposed to binding via dispersion and ionic forces. What this implies is that ixosin B (and other AMPs) has the potential to generate "non-transient" pores due to the increased residence time in the membrane. Although this may not lead to cell death directly, it gives other antimicrobial effectors continued access to the bacteria, a scenario whereby bacterial recovery is virtually impossible. It should also be noted that ROS formation by Cu−ATCUN complexes is highly catalytic.[38] This means that even a small amount of copper-bound ixosin has the potential to elicit the same biological effect.

Conclusions. AMPs represent a large class of molecules that multicellular organisms use for defense against pathogens. Considered as one of nature's oldest antibiotics, AMPs rely on their overall positive charge and conformational plasticity to recognize multiple targets and have broad-spectrum activities. Many modes of action have been proposed and proven for a

DOI: 10.1021/acsinfecdis.5b00140
ACS Infect. Dis. 2016, 2, 71−81

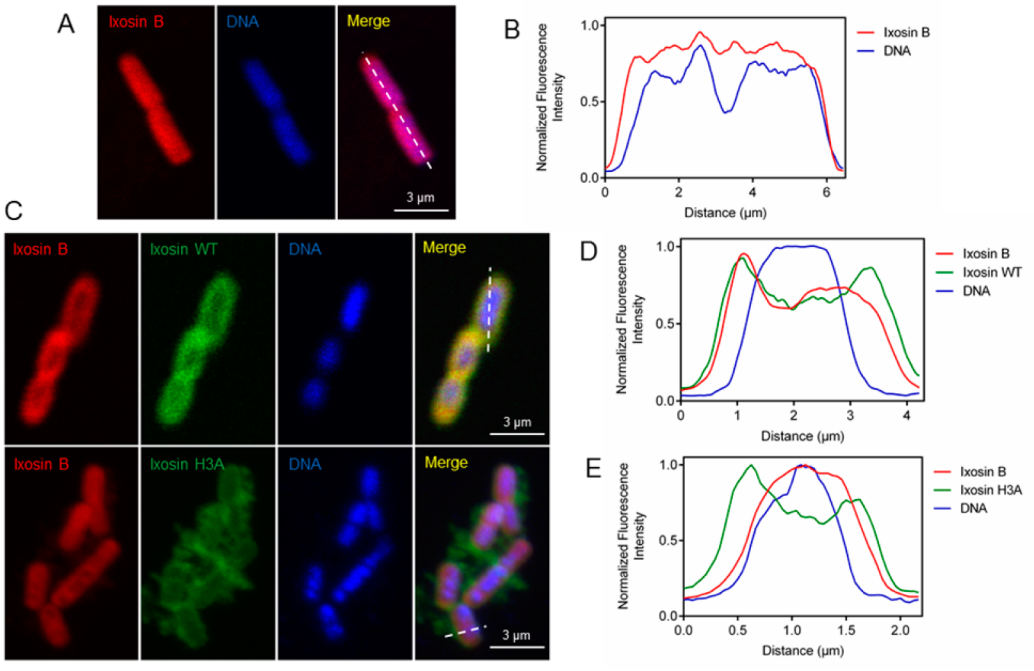

Figure 5. ATCUN motif in ixosin increases ixosin B affinity to the bacterial membrane: (A) localization of TAMRA−ixosin B and (B) fluorescence intensity curves showing ixosin B co-localizing with bacterial nucleoid; (C) co-localization studies of *E. coli* MWF1 cotreated with ixosin (WT and H3A) and ixosin B; (D) increased localization of ixosin B to the bacterial periphery upon simultaneous treatment with ixosin WT and ixosin B; (E) restoration of normal co-localization of ixosin B with DNA when cells are cotreated with ixosin H3A. Axes used to obtain fluorescence intensities are shown as broken white lines in the merge panels.

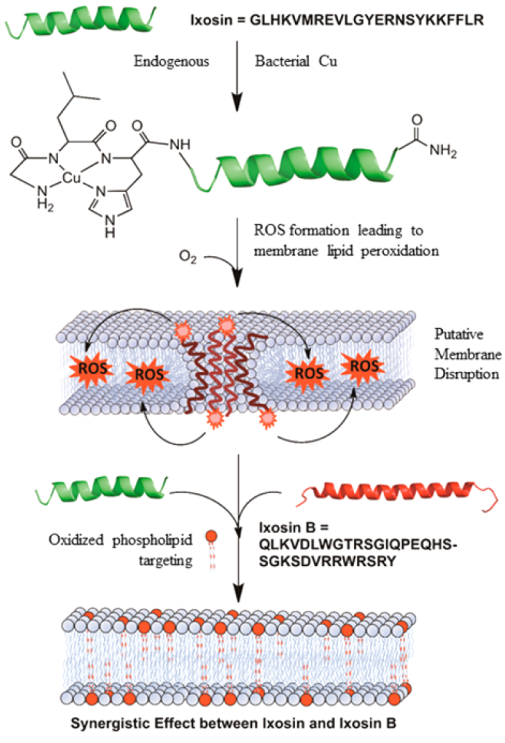

Figure 6. Proposed mechanism of antimicrobial activity of ixosin and its synergy with ixosin B. Both peptides are depicted as helical, and ixosin is shown to form toroidal pores in the membrane for illustration purposes only.

large number of AMPs, most of which converge on the idea that AMPs bind electrostatically to the anionic bacterial membrane, induce local perturbations, and generate pores. In addition, AMPs have been found to translocate across the membrane and inhibit intracellular processes including protein and DNA synthesis.[20,25] This seemingly diverse mechanism of action can be intuitively attributed to the AMP's inherent flexibility, allowing it to recognize a wide variety of targets. Regardless of the mechanism, three distinct physical properties seem to dictate a peptide's biological activity: amphipathicity, hydrophobicity, and cationic charge. Herein, we study the molecular determinants to ixosin's bioactivity and find that it is, indeed, in part dictated by its hydrophobicity and positive charge. Although largely unexplored in this study, ixosin, much like any canonical AMP (due to its membrane affinity) may also generate membrane pores. We focused on the contribution of the copper-binding motif (Gly_1-Leu_2-His_3) to the biological activity of Ixosin. Our findings reveal that the ATCUN motif GLH confers bactericidal properties to ixosin at its MIC. The affinity of ixosin for the bacterial membrane allows the ATCUN motif in ixosin to produce oxidative damage to the membrane lipid unsaturation in a copper- and oxygen-dependent manner. Once the lipids are (per)oxidized, it paves the way for other AMPs to act synergistically via an unknown mechanism. Taken altogether, our results indicate that there are at least two modes of action by ixosin−membrane binding/disruption (from the hydrophobic and positively charged portion) and membrane oxidation (from the ATCUN domain). We believe the two domains likely act in a cooperative fashion (as highlighted by the synergy between ixosin WT and ixosin H3A) and that the ATCUN motif requires the rest of the peptide to generate its full oxidative effect. From a molecular standpoint, this may represent economic efficiency and an evolutionary advantage because the tick expressing ixosin gets multiple modes of action from a single molecule, allowing it to combat a deluge of microorganisms. Herein, we present an undocumented case of

DOI: 10.1021/acsinfecdis.5b00140
ACS Infect. Dis. 2016, 2, 71−81

an AMP acting in concert with Cu^{2+} to generate oxidative effects as part of its mechanism of action and as a key element for its synergy with ixosin B—another AMP expressed in the same tick gland. Surely AMPs and other antimicrobial effectors—no matter how seemingly unrelated they are—exhibit a dynamic interplay to generate a quick, amplified, and effective immune response. This paradigm is becoming more apparent in recent literature.

The fact that ATCUN-containing AMPs have been isolated from very diverse forms of life may represent a generalized defense mechanism from unrelated organisms. Of special relevance to this is that metchnikowin, an ATCUN-containing AMP from *Drosophila*, has been shown to be induced constitutively in response to any microbial challenge (Gram ± and fungi), whereas other AMPs (e.g., diptericin, cecropin A, and drosocin) have been induced only selectively.[53] It is tantalizing to assume that the ATCUN-containing AMPs may be a point of convergence for most AMPs because their capability to form ROS may sensitize microbes to attack by other AMPs. In particular, *Borrelia burgdorferi*, the causative agent of Lyme disease transmitted by ticks, possess membranes enriched with polyunsaturated fatty acids that are particularly sensitive to attack by ROS.[54] Our study also reveals another avenue by which tick AMPs utilize copper in their activity (much like microplusin[6]) at the same time, unifying it with ROS production (like hemoglobin fragments[5]). Although we are unsure of the molecular details of their synergy, our results may have important ramifications in the understanding of the tick innate immune response, more specifically a possible reason for its vector competence.

METHODS

Antimicrobial Assay. Antimicrobial susceptibility testing was done using the broth microdilution method as suggested by Hancock.[55] Gram-positive *Staphylococcus aureus* (ATCC 25923); and Gram-negative *Escherichia coli* (DL7) and *Pseudomonas aeruginosa* (PAO1) were grown in Mueller–Hinton broth (MHB, Difco) until mid-log phase for 3–5 h. The fungus *Candida albicans* was grown in yeast mold broth. Peptide stock solutions were diluted in PBS (Gibco), pH 7.40, and 50 μL 2-fold serial dilutions (starting from 32 μM) were placed on a sterile 96-well poplypropylene plate (Greiner). To each well was added 50 μL of a bacterial suspension, resulting in a final inoculum of 5×10^5 CFU/mL per well. Ampicillin (Sigma-Aldrich) was used as positive control and PBS as negative control. Plates were incubated at 37 °C for 18–20 h. MIC was defined as the concentration that prevented visual growth of bacteria. MICs reported here are the mode of three independent trials. To test synergy between ixosin and ixosin B, a 1:1 molar ratio of peptides was mixed and added to a culture of *E. coli* PDJ1 and *E. coli* MWF1. The FIC index was calculated using the formula FIC index = $([A]_{mix}/\text{MIC A}) + ([B]_{mix}/\text{MIC B})$. A FIC index < 0.5 indicates good synergy (a 4-fold increase in MIC in combination) and a FIC index = 1.0 indicates additive effects.

Nuclear Magnetic Resonance Studies. NMR data were collected at 25 °C on an Agilent (Varian) INOVA 600 MHz NMR spectrometer equipped with a cold probe. The standard BioPack pulse sequences were used. The NMR sample of 2.3 mM unlabeled ixosin in 20 mM acetate buffer at pH 4.4, 7% D_2Oi was used to obtain the sequence-specific chemical shift assignment of the NMR resonances. For this, a set of spectra was collected and analyzed: 2D $^1H-^{15}N$ HSQC, $^1H-^{13}C$ HSQC, $^1H-^1H$ TOCSY (mixing time = 0.07 s) and NOESY (mixing time = 0.15 s) and 3D ^{15}N-edited TOCSY (mixing time = 0.07 s) and NOESY (mixing time = 0.3 s). The spectra were processed with NMRPipe[56] and analyzed by CCPNMR[57] analysis. The binding of Cu^{2+} to ixosin was studied by HSQC titration approach. The NMR signals from nuclei participating in coordination with a metal will disappear from the HSQC spectrum due to deprotonation. In addition, because Cu^{2+} exhibits paramagnetic properties, the NMR signals of peptide nuclei adjacent to the metal coordination site will experience a broadening and decrease of their intensities compared to the free peptide spectra. Thus, to identify the metal binding site, the NMR sample of unlabeled ixosin was titrated with $CuCl_2$, and $^1H-^{15}N$ and $^1H-^{13}C$ HSQC spectra were collected at stoichiometric ratios 5:1, 2:1, 1:1, 1:2, and 1:5.

Confocal Fluorescence Microscopy Imaging. Images were acquired on a Nikon A1R spectral confocal microscope using a 100× oil immersion objective at a pixel resolution of 1024 × 1024. *E. coli* MG1655 was labeled by incubation with 5(6)-carboxyfluorescein-labeled peptides at the MIC for 30 min. The cells were then pelleted and resuspended in PBS prior to imaging. For co-localization studies, the same treatment was done except that *E. coli* MWF1 strain was used. Fluorescence intensity was obtained from micrograph analysis using ImageJ.

Activity of Ixosin in O_2- and Cu^{2+}-Starved Conditions. Fifty microliters of a 10^6 CFU/mL bacterial (*E. coli* MG1655) suspension (in 5 mM HEPES, 100 mM KCl, 5 mM glucose, pH 7.30) was mixed with 50 μL of peptide at 2 times its MIC. The resulting mixture was split into two 50 μL aliquots, one of which was incubated in a 37 °C incubator and the other was placed in a gastight anaerobic chamber at the same temperature. After 2 h, 1000-fold dilutions were plated onto LB agar plates and allowed to grow overnight. For the copper chelation experiments, the same manipulations were done except that the cells were cotreated with 200 μM triethylenetetramine or 50 μM penicillamine. Colonies were counted manually, and the bars represent the mean ± SEM from three independent trials.

Lipid Peroxidation Assay.[58] *E. coli* strain MWF1, *fabR::kan recD::Tn10* (containing a higher level of unsaturated fatty acid in its membrane) was grown, washed, and resuspended in 20 mM HEPES, 100 mM NaCl, pH 7.40, and was incubated with peptides at their MIC without addition of exogenous Cu^{2+} for 2 h. Then, the suspension was subjected to a standard thiobarbituric acid (TBA) assay to determine the amount of peroxidation product. Briefly, 50 μL of treated bacteria was added to 150 μL of $HClO_4$ and 150 μL of 40 mM TBA. The mixture was heated in a dry block for 60 min at 97 °C followed by a 20 min cool down at −20 °C. Then, 300 μL of methanol and 100 μL of 20% trichloroacetic acid were added. A 100 μL aliquot was injected in a C_{18} analytical column and eluted at 1 mL/min (for 15 min) using 72:17:11 50 mM KH_2PO_4 pH 7:MeOH:ACN. Ninety-seven percent tetramethoxypropane (Sigma) at different concentrations was used as external standard to quantify micromoles of TBARS. Bars represent the mean ± SEM obtained from three independent trials.

Tryptophan Fluorescence Quenching. LUVs composed of 3:1 POPE:DOPG were prepared, and a sample was preoxidized with 100 μM Cu–ixosin WT and 1 mM ascorbate for 36 h. Ixosin B was added to native or oxidized LUVs to a final concentration of 20 μM (with LUV at 200 μM). Initial fluorescence was recorded using a Varian Cary50 spectrofluorometer with excitation set at 295 nm, emission at 310–390

DOI: 10.1021/acsinfecdis.5b00140
ACS Infect. Dis. 2016, 2, 71–81

nm, and PMT voltage at 650. Then a small aliquot of acrylamide was titrated into the mixture with subsequent recording of fluorescence quenching. Points represent the mean ± SEM from three independent experiments obtained from different LUV preparations.

Statistical Analysis. Data were analyzed for statistical differences using Graph-Pad Prism v6.0 software. One-way or two-way ANOVA was used to determine statistical significance and was set at $P < 0.05$.

■ ASSOCIATED CONTENT

Supporting Information

The Supporting Information is available free of charge on the ACS Publications website at DOI: 10.1021/acsinfecdis.5b00140.

Figures S1−S10 and Tables S1 and S2 as well as other experimental procedures (PDF)

■ AUTHOR INFORMATION

Corresponding Author

*(A.M.A.-B.) E-mail: alfredo.angeles-boza@uconn.edu.

Notes

The authors declare no competing financial interest.

■ ACKNOWLEDGMENTS

A.M.A.-B. acknowledges the University of Connecticut for startup funds. We are grateful to Prof. Kenneth G. Campellone and Dr. Jorge Cervantes for the generous gifts of HeLa and HEK293 cells, respectively.

■ REFERENCES

(1) Hancock, R. E., and Sahl, H. G. (2006) Antimicrobial and host-defense peptides as new anti-infective therapeutic strategies. *Nat. Biotechnol. 24*, 1551−1557.

(2) Zasloff, M. (2002) Antimicrobial peptides of multicellular organisms. *Nature 415*, 389−395.

(3) Hajdusek, O., Sima, R., Ayllon, N., Jalovecka, M., Perner, J., de la Fuente, J., and Kopacek, P. (2013) Interaction of the tick immune system with transmitted pathogens. *Front. Cell. Infect. Microbiol. 3*, 26.

(4) Tonk, M., Cabezas-Cruz, A., Valdes, J. J., Rego, R. O., Grubhoffer, L., Estrada-Pena, A., Vilcinskas, A., Kotsyfakis, M., and Rahnamaeian, M. (2015) *Ixodes ricinus* defensins attack distantly-related pathogens. *Dev. Comp. Immunol. 53*, 358−365.

(5) Smith, A. A., and Pal, U. (2014) Immunity-related genes in *Ixodes scapularis* − perspectives from genome information. *Front. Cell. Infect. Microbiol. 4*, 116.

(6) Silva, F. D., Rezende, C. A., Rossi, D. C., Esteves, E., Dyszy, F. H., Schreier, S., Gueiros-Filho, F., Campos, C. B., Pires, J. R., and Daffre, S. (2009) Structure and mode of action of microplusin, a copper II-chelating antimicrobial peptide from the cattle tick *Rhipicephalus (Boophilus) microplus*. *J. Biol. Chem. 284*, 34735−34746.

(7) Horn, M., Nussbaumerova, M., Sanda, M., Kovarova, Z., Srba, J., Franta, Z., Sojka, D., Bogyo, M., Caffrey, C. R., Kopacek, P., and Mares, M. (2009) Hemoglobin digestion in blood-feeding ticks: mapping a multipeptidase pathway by functional proteomics. *Chem. Biol. 16*, 1053−1063.

(8) Cruz, C. E., Fogaca, A. C., Nakayasu, E. S., Angeli, C. B., Belmonte, R., Almeida, I. C., Miranda, A., Miranda, M. T., Tanaka, A. S., Braz, G. R., Craik, C. S., Schneider, E., Caffrey, C. R., and Daffre, S. (2010) Characterization of proteinases from the midgut of *Rhipicephalus (Boophilus) microplus* involved in the generation of antimicrobial peptides. *Parasites Vectors 3*, 63.

(9) Francischetti, I. M., Sa-Nunes, A., Mans, B. J., Santos, I. M., and Ribeiro, J. M. (2009) The role of saliva in tick feeding. *Front. Biosci., Landmark Ed. 14*, 2051−2088.

(10) Yu, D., Sheng, Z., Xu, X., Li, J., Yang, H., Liu, Z., Rees, H. H., and Lai, R. (2006) A novel antimicrobial peptide from salivary glands of the hard tick, *Ixodes sinensis*. *Peptides 27*, 31−35.

(11) Lehrer, R. I., and Lu, W. (2012) α-Defensins in human innate immunity. *Immunol. Rev. 245*, 84−112.

(12) Harford, C. S. B. (1997) Amino terminal Cu(II)- and Ni(II)-binding (ATCUN) motif of proteins and peptides: metal binding, DNA cleavage, and other properties. *Acc. Chem. Res. 30*, 123−130.

(13) Park, C. J., Park, C. B., Hong, S. S., Lee, H. S., Lee, S. Y., and Kim, S. C. (2000) Characterization and cDNA cloning of two glycine- and histidine-rich antimicrobial peptides from the roots of shepherd's purse, *Capsella bursa-pastoris*. *Plant Mol. Biol. 44*, 187−197.

(14) Mitta, G., Hubert, F., Noel, T., and Roch, P. (1999) Myticin, a novel cysteine-rich antimicrobial peptide isolated from haemocytes and plasma of the mussel *Mytilus galloprovincialis*. *Eur. J. Biochem. 265*, 71−78.

(15) Lee, I. H., Zhao, C., Cho, Y., Harwig, S. S., Cooper, E. L., and Lehrer, R. I. (1997) Clavanins, α-helical antimicrobial peptides from tunicate hemocytes. *FEBS Lett. 400*, 158−162.

(16) Silphaduang, U., and Noga, E. J. (2001) Peptide antibiotics in mast cells of fish. *Nature 414*, 268−269.

(17) Peng, K. C., Lee, S. H., Hour, A. L., Pan, C. Y., Lee, L. H., and Chen, J. Y. (2012) Five different piscidins from Nile tilapia, *Oreochromis niloticus*: analysis of their expressions and biological functions. *PLoS One 7*, e50263.

(18) Wu, Y., Wang, L., Zhou, M., Ma, C., Chen, X., Bai, B., Chen, T., and Shaw, C. (2011) Limnonectins: a new class of antimicrobial peptides from the skin secretion of the Fujian large-headed frog (*Limnonectes fujianensis*). *Biochimie 93*, 981−987.

(19) Perrin, B. S., Jr., Tian, Y., Fu, R., Grant, C. V., Chekmenev, E. Y., Wieczorek, W. E., Dao, A. E., Hayden, R. M., Burzynski, C. M., Venable, R. M., Sharma, M., Opella, S. J., Pastor, R. W., and Cotten, M. L. (2014) High-resolution structures and orientations of antimicrobial peptides piscidin 1 and piscidin 3 in fluid bilayers reveal tilting, kinking, and bilayer immersion. *J. Am. Chem. Soc. 136*, 3491−3504.

(20) Hayden, R. M., Goldberg, G. K., Ferguson, B. M., Schoeneck, M. W., Libardo, M. D. J., Mayeux, S. E., Shrestha, A., Bogardus, K. A., Hammer, J., Pryshchep, S., Lehman, H. K., McCormick, M., Blazyk, J., Angeles-Boza, A. M., Fu, R., and Cotten, M. L. (2015) Complementary effects of host defense peptides piscidin 1 and piscidin 3 on DNA and lipid membranes: biophysical insights into contrasting biological activities. *J. Phys. Chem. B 119*, 15235−15246.

(21) Libardo, M. D., Cervantes, J. L., Salazar, J. C., and Angeles-Boza, A. M. (2014) Improved bioactivity of antimicrobial peptides by addition of amino-terminal copper and nickel (ATCUN) binding motifs. *ChemMedChem 9*, 1892−1901.

(22) Libardo, M. D., Nagella, S., Lugo, A., Pierce, S., and Angeles-Boza, A. M. (2015) Copper-binding tripeptide motif increases potency of the antimicrobial peptide anoplin via reactive oxygen species generation. *Biochem. Biophys. Res. Commun. 456*, 446−451.

(23) Libardo, M. D., Paul, T. J., Prabhakar, R., and Angeles-Boza, A. M. (2015) Hybrid peptide ATCUN-sh-Buforin: influence of the ATCUN charge and stereochemistry on antimicrobial activity. *Biochimie 113*, 143−155.

(24) Joyner, J. C., Hodnick, W. F., Cowan, A. S., Tamuly, D., Boyd, R., and Cowan, J. A. (2013) Antimicrobial metallopeptides with broad nuclease and ribonuclease activity. *Chem. Commun. (Cambridge, U. K.) 49*, 2118−2120.

(25) Brogden, K. A. (2005) Antimicrobial peptides: pore formers or metabolic inhibitors in bacteria? *Nat. Rev. Microbiol. 3*, 238−250.

(26) Fjell, C. D., Hiss, J. A., Hancock, R. E., and Schneider, G. (2012) Designing antimicrobial peptides: form follows function. *Nat. Rev. Neurosci. 11*, 37−51.

(27) Bohm, G., Muhr, R., and Jaenicke, R. (1992) Quantitative analysis of protein far UV circular dichroism spectra by neural networks. *Protein Eng., Des. Sel. 5*, 191−195.

(28) Koval, I. A., van der Schilden, K., Schuitema, A. M., Gamez, P., Belle, C., Pierre, J. L., Luken, M., Krebs, B., Roubeau, O., and Reedijk, J. (2005) Proton NMR spectroscopy and magnetic properties of a

DOI: 10.1021/acsinfecdis.5b00140
ACS Infect. Dis. 2016, 2, 71−81

solution-stable dicopper(II) complex bearing a single mu-hydroxo bridge. *Inorg. Chem. 44*, 4372−4382.
(29) Last, N. B., Schlamadinger, D. E., and Miranker, A. D. (2013) A common landscape for membrane-active peptides. *Protein Sci. 22*, 870−882.
(30) Nguyen, L. T., Haney, E. F., and Vogel, H. J. (2011) The expanding scope of antimicrobial peptide structures and their modes of action. *Trends Biotechnol. 29*, 464−472.
(31) Cudic, M., and Otvos, L., Jr. (2002) Intracellular targets of antibacterial peptides. *Curr. Drug Targets 3*, 101−106.
(32) Bechara, C., and Sagan, S. (2013) Cell-penetrating peptides: 20 years later, where do we stand? *FEBS Lett. 587*, 1693−1702.
(33) Park, C. B., Yi, K. S., Matsuzaki, K., Kim, M. S., and Kim, S. C. (2000) Structure-activity analysis of buforin II, a histone H2A-derived antimicrobial peptide: the proline hinge is responsible for the cell-penetrating ability of buforin II. *Proc. Natl. Acad. Sci. U. S. A. 97*, 8245−8250.
(34) Falla, T. J., Karunaratne, D. N., and Hancock, R. E. (1996) Mode of action of the antimicrobial peptide indolicidin. *J. Biol. Chem. 271*, 19298−19303.
(35) Hsu, C. H., Chen, C., Jou, M. L., Lee, A. Y., Lin, Y. C., Yu, Y. P., Huang, W. T., and Wu, S. H. (2005) Structural and DNA-binding studies on the bovine antimicrobial peptide, indolicidin: evidence for multiple conformations involved in binding to membranes and DNA. *Nucleic Acids Res. 33*, 4053−4064.
(36) Jin, Y., and Cowan, J. A. (2005) DNA cleavage by copper-ATCUN complexes. Factors influencing cleavage mechanism and linearization of dsDNA. *J. Am. Chem. Soc. 127*, 8408−8415.
(37) Jin, Y., Lewis, M. A., Gokhale, N. H., Long, E. C., and Cowan, J. A. (2007) Influence of stereochemistry and redox potentials on the single- and double-strand DNA cleavage efficiency of Cu(II) and Ni(II) Lys-Gly-His-derived ATCUN metallopeptides. *J. Am. Chem. Soc. 129*, 8353−8361.
(38) Joyner, J. C., Reichfield, J., and Cowan, J. A. (2011) Factors influencing the DNA nuclease activity of iron, cobalt, nickel, and copper chelates. *J. Am. Chem. Soc. 133*, 15613−15626.
(39) Roversi, D., Luca, V., Aureli, S., Park, Y., Mangoni, M. L., and Stella, L. (2014) How many antimicrobial peptide molecules kill a bacterium? The case of PMAP-23. *ACS Chem. Biol. 9*, 2003−2007.
(40) Fernandez-Mazarrasa, C., Mazarrasa, O., Calvo, J., del Arco, A., and Martinez-Martinez, L. (2009) High concentrations of manganese in Mueller-Hinton agar increase MICs of tigecycline determined by Etest. *J. Clin. Microbiol. 47*, 827−829.
(41) Helbig, K., Bleuel, C., Krauss, G. J., and Nies, D. H. (2008) Glutathione and transition-metal homeostasis in *Escherichia coli*. *J. Bacteriol. 190*, 5431−5438.
(42) Outten, F. W., and Munson, G. P. (2013) Lability and liability of endogenous copper pools. *J. Bacteriol. 195*, 4553−4555.
(43) Fung, D. K., Lau, W. Y., Chan, W. T., and Yan, A. (2013) Copper efflux is induced during anaerobic amino acid limitation in *Escherichia coli* to protect iron-sulfur cluster enzymes and biogenesis. *J. Bacteriol. 195*, 4556−4568.
(44) Fu, Y., Chang, F. M., and Giedroc, D. P. (2014) Copper transport and trafficking at the host-bacterial pathogen interface. *Acc. Chem. Res. 47*, 3605−3613.
(45) Choi, K. Y., Chow, L. N., and Mookherjee, N. (2012) Cationic host defence peptides: multifaceted role in immune modulation and inflammation. *J. Innate Immun. 4*, 361−370.
(46) Hilchie, A. L., Wuerth, K., and Hancock, R. E. (2013) Immune modulation by multifaceted cationic host defense (antimicrobial) peptides. *Nat. Chem. Biol. 9*, 761−768.
(47) Liu, Z., Liu, H., Liu, X., and Wu, X. (2008) Purification and cloning of a novel antimicrobial peptide from salivary glands of the hard tick, *Ixodes sinensis*. *Comp. Biochem. Physiol., Part B: Biochem. Mol. Biol. 149*, 557−561.
(48) Hong, R., Kang, T. Y., Michels, C. A., and Gadura, N. (2012) Membrane lipid peroxidation in copper alloy-mediated contact killing of *Escherichia coli*. *Appl. Environ. Microbiol. 78*, 1776−1784.
(49) Mattila, J. P., Sabatini, K., and Kinnunen, P. K. (2008) Oxidized phospholipids as potential molecular targets for antimicrobial peptides. *Biochim. Biophys. Acta, Biomembr. 1778*, 2041−2050.
(50) Steinbrecher, U. P. (1987) Oxidation of human low density lipoprotein results in derivatization of lysine residues of apolipoprotein B by lipid peroxide decomposition products. *J. Biol. Chem. 262*, 3603−3608.
(51) Kurvinen, J. P., Kuksis, A., Ravandi, A., Sjovall, O., and Kallio, H. (1999) Rapid complexing of oxoacylglycerols with amino acids, peptides and aminophospholipids. *Lipids 34*, 299−305.
(52) Rozga, M., Sokolowska, M., Protas, A. M., and Bal, W. (2007) Human serum albumin coordinates Cu(II) at its N-terminal binding site with 1 pM affinity. *JBIC, J. Biol. Inorg. Chem. 12*, 913−918.
(53) Lemaitre, B., Reichhart, J. M., and Hoffmann, J. A. (1997) *Drosophila* host defense: differential induction of antimicrobial peptide genes after infection by various classes of microorganisms. *Proc. Natl. Acad. Sci. U. S. A. 94*, 14614−14619.
(54) Boylan, J. A., Lawrence, K. A., Downey, J. S., and Gherardini, F. C. (2008) *Borrelia burgdorferi* membranes are the primary targets of reactive oxygen species. *Mol. Microbiol. 68*, 786−799.
(55) Wiegand, I., Hilpert, K., and Hancock, R. E. (2008) Agar and broth dilution methods to determine the minimal inhibitory concentration (MIC) of antimicrobial substances. *Nat. Protoc. 3*, 163−175.
(56) Delaglio, F., Grzesiek, S., Vuister, G. W., Zhu, G., Pfeifer, J., and Bax, A. (1995) NMRPipe: a multidimensional spectral processing system based on UNIX pipes. *J. Biomol. NMR 6*, 277−293.
(57) Vranken, W. F., Boucher, W., Stevens, T. J., Fogh, R. H., Pajon, A., Llinas, M., Ulrich, E. L., Markley, J. L., Ionides, J., and Laue, E. D. (2005) The CCPN data model for NMR spectroscopy: development of a software pipeline. *Proteins: Struct., Funct., Genet. 59*, 687−696.
(58) Boylan, J. A., and Gherardini, F. C. (2008) Determining the cellular targets of reactive oxygen species in *Borrelia burgdorferi*. *Methods Mol. Biol. 431*, 213−221.

DOI: 10.1021/acsinfecdis.5b00140
ACS Infect. Dis. 2016, 2, 71−81